Accepted Manuscript

Mesogenic heterocycles derived from quinoxaline Schiff Bases

Hsiu-Ming Kuo, Wan-Ping Ko, Gene-Hsiang Lee, Chung K. Lai

PII: S0040-4020(16)30747-5

DOI: 10.1016/j.tet.2016.07.076

Reference: TET 27972

To appear in: *Tetrahedron*

Received Date: 15 May 2016

Revised Date: 17 July 2016

Accepted Date: 30 July 2016

Please cite this article as: Kuo H-M, Ko W-P, Lee G-H, Lai CK, Mesogenic heterocycles derived from quinoxaline Schiff Bases, *Tetrahedron* (2016), doi: 10.1016/j.tet.2016.07.076.

Mesogenic Heterocycles Derived from Quinoxaline Schiff Bases

Hsiu–Ming Kuo, Wan–Ping Ko, Gene–Hsiang Lee, Chung K. Lai*

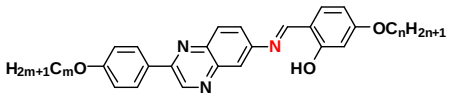

1; m, n = 8, 10, 12

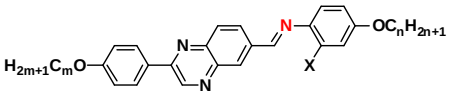

2a; X = OH, m = 12, n = 8, 12, 16
2b: X = H, m = 12, n = 8, 12, 16

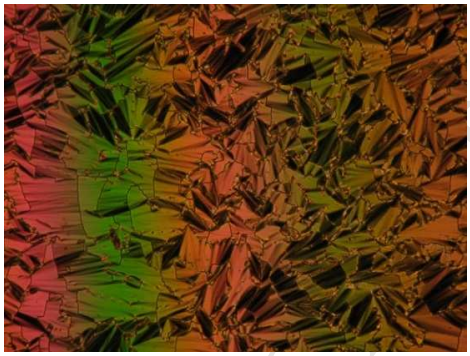

Mesogenic Heterocycles Derived from Quinoxaline Schiff Bases

Hsiu–Ming Kuo, Wan-Ping Ko, Gene–Hsiang Lee, Chung K. Lai*

Department of Chemistry, National Central University, Chung-Li, Taiwan, ROC

Abstract.

Three new series of heterocyclic quinoxaline Schiff Bases **1**-**2** were prepared, characterized and their mesomorphic properties were investigated. These compounds **1** and **2** are in fact geometric isomers in which an imine moiety (e.g. –C=N) is inversely incorporated into quinoxaline, leading to an opposite local dipole. Two single crystallographic structures **1** (m = 8, n = 8) and **2a** (m = 12, n = 8) were determined by X–ray crystallographic analysis in order to understand the effect of mesomorphic properties. Weak H–bonds, CH–π and π–π interactions were found in both crystals, which were attributed to the formation of mesomorphic behavior. Variable temperature FT–IR experiments were performed to confirm the induced H–bonds. All series series of compounds **1**–**2** exhibited N/SmC or SmC phases, which were identified by optical microscope and confirmed by powder X–ray diffraction experiments. Compounds **2a** have a slightly wider range of mesophase temperatures than that of compounds **1** and **2b**.

* Corresponding author. Tel.: +886 03 4259207; fax: +886 03 4277972
e–Mail address: cklai@cc.ncu.edu.tw (C.K. Lai).

1. Introduction

An exquisite balance of molecular interactions in mesogenic structures is crucially important to the formation of a preferred arrangement in order to generate practical materials with cooperative properties. Dipole is one of the forces or interactions that have been commonly utilized in the design of liquid crystalline materials. Such dipole or polarization might be intrinsically existent or induced under an external influence. Intrinsic dipoles are generally obtained from molecular structures when designed properly. A polar group incorporated resulting in an asymetric structure is a common approach. This is particularly important in rod–shaped molecules. Rod–like molecule has an elongated and anisotropic geometry which allows for preferential alignments along one spatial direction. On the other hand, too strong or too weak an interaction force often resulted in the formation of a solid or liquid state. However, such a force balance seems to be almost impossible to control and predict.

Schiff bases, such as salicyladimine and enaminoketone[1] were probably the most studied among known mesogens due to their known chemistry and versatile structures. They were easily prepared by condensations of ketones or aldehydes with amines. The Schiff bases were constructed by an imine moiety (–C=N). The imine fragment not only plays a role of linking group, but also holds a local dipole moment. On the other hand, this dipole might macroscopically induce the overall liquid crystallinity if incorporated correctly. In addition, the better planarity of salicylaldimines derivatives formed by intramolecular H–bond often facilitated a more ordered or preferred arrangement in mesophases.

Quinoxalines, considered as a heterocyclic core moiety have been applied to produce photo luminecent and/ or efficient electroluminescent materials[2] due to their extended π–conjugated and more rigid structures. It is an electron–transporting or hole–blocking layer in organic light-emitting diodes[3] (OLEDs) because of its relative ease of preparation and also higher thermal stability. Known examples of mesogenic quinoxalines[4] were relatively rare, and the formation of mesophases was mostly attributed to the weak intermolecular π–π interactions. A

good LC gelator obtained from dibenzophenazine and diphenylquinoxaline[5] was observed and studied. Interestingly, a double–decked, hydrophobic metallocyclophane[6] was formed by self–assemble of quinoxaline–pyridine hybrids with tetrahedral metals (i.e. Cu^{1+}, Ag^{1+}). A similar series of N-salicylidene-2-hydroxyanilines[7] **I** and quinoxaline–salicylaldimine conjugates **II** were previously prepared in this group (Fig. 1). All compounds **I** formed an enantitropic SmC phase, compounds **II** formed an enantiotropic columnar phase. This is the first examples derived from N-salicylidene-2-hydroxy aniline that exhibited columnar phases. A series of electron–accepting acene–type LC materials, dialkoxycyano pyrazinoquinoxaline[8] **III** were also developed, and its hole mobility in SmA phase was observed. In these highly conjugated systems, CH–π and π–π interactions[9] also played an important role.

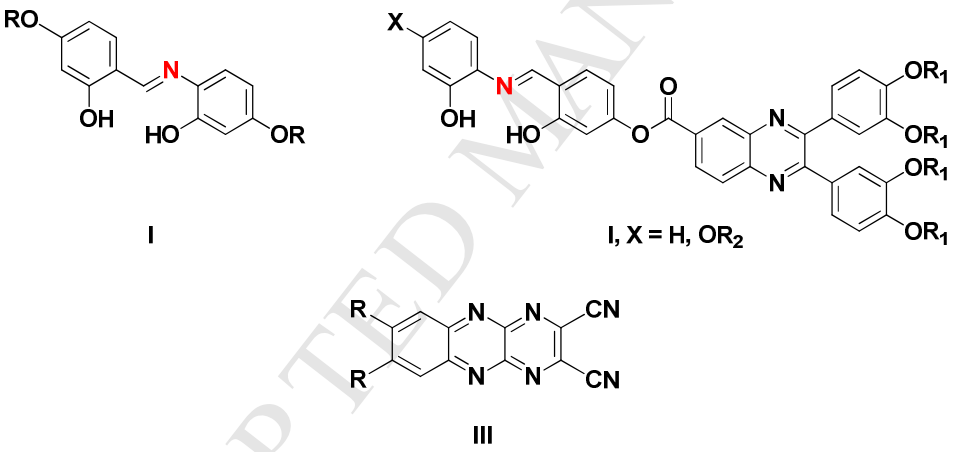

Fig. 1 The molecular structures of similar compounds **I**–**III**.

In this work, three series of Schiff Bases **1**–**2** (see Scheme 1) incorporating heterocyclic quinoxaline were prepared, characterized and their mesomorphic properties were investigated. These compounds; iminephenols **1** and aminophenols **2a** are in fact geometric isomers in which an inime moiety (e.g. –C=N) is inversely incorporated. Dipole induced in opposite direction might impact the overall dipole generated in these two series of rod–like molecules. A systematic investigation of the structure–property relationship by changing the terminal carbon lengths and the dipole might provide us about microscopic and/or macroscopic information in

understanding the relationship between the structures and the properties. Compound **2b** was also prepared to understand the effect of H–bonds formed by hydroxyl group on the formation of mesomorphic behavior. Single crystal crystallographic data of two single crystals showed that the intramolecular and intermolecular H–bonds were observed in the crystal phases. Variable temperature FT–IR experiments were performed to confirm the H–bonds induced in crystal phases. Results indicated that all compounds **1**–**2** were truly mesogenic, exhibiting nematic/smectic C or smectic C phases, which were identified and confirmed by powder X–ray diffraction. The UV–vis absorption and PL spectra of three compounds in CH_2Cl_2 solution at room temperature were also studied.

2. Results and Discussion

2.1 Synthesis and Characterization

The synthetic procedures for compounds **1** are summarized in Scheme 1. 2-(4-Hydroxy phenyl)-2-oxoacetaldehyde was prepared by the reaction of 1-(4-hydroxyphenyl)ethanone and SeO_2 in refluxing 1,4-dioxane/H_2O. Methyl 2-(4-hydroxyphenyl)quinoxaline-6-carboxylate was obtained by the reaction of 3,4-diaminobenzoate with 2-(4-hydroxyphenyl)-2-oxoacetaldehyde in refluxing ethanol. Alkylation of methyl 2-(4-hydroxyphenyl)quinoxaline-6-carboxylate with *n*-alkylbromides and K_2CO_3 in refluxing acetone gave 2-(4-alkoxyloxyphenyl)quinoxaline-6-carboxylates, which were then further reduced by Pd/C and hydrazine monohydrate to produce 2-(4-(alkoxy)phenyl)quinoxalin-6-amines. All amines were freshly prepared and directly used for the final steps without any purification. The final compounds **1**, (E)-5-(alkoxy)-2-(((2-(4-(alkoxy)phenyl)quinoxalin-6-yl) imino)methyl)phenols were obtained by reaction of 2-hydroxy-4-(alkoxy)benzaldehydes and 2-(4-(alkoxy)phenyl)quinoxalin-6-amines in refluxing dried THF. ^{1}H and ^{13}C NMR spectroscopy in $CDCl_3$ were used to characterize all intermediates. For instance, two characteristic singlet peaks occurred at δ 8.67–8.68 and 13.40–13.51 ppm, were assigned for imine –CH=N and phenolic –OH groups in compounds **1**.

The synthetic procedures for compounds **2** are summarized in Scheme 2. Methyl 2-(4-hydroxyphenyl)quinoxaline-6-carboxylates and methyl 2-(4-(alkoxy)phenyl)quinoxaline-6-carboxylates were prepared similar to aforementioned procedures in Scheme 1 for methyl 2-(4-hydroxyphenyl)quinoxaline-6-carboxylate and 2-(4-alkoxyloxyphenyl)quinoxaline-6-carboxylates. (2-(4-(Alkoxy)phenyl)quinoxalin-6-yl)methanols were obtained by reduction of methyl 2-(4-(alkoxy)phenyl)quinoxaline-6-carboxylates with LAH stirring in THF. Then 2-(4-(alkoxy)phenyl)quinoxaline-6-carbaldehydes were prepared by oxidation of (2-(4-(alkoxy) phenyl)quinoxalin-6-yl)methanols with pyridinium chlorochromate in stirring THF. Two characteristic singlet peaks on ^{1}H-NMR spectroscopic spectra occurred at δ 4.91and 10.23 ppm, assigned for groups –CH_2OH and –C*H*O. The final compounds **2a** and **2b** were obtained by condensation reactions of 2-(4-(Alkoxy)phenyl)quinoxaline-6-carbaldehydes with appropriate amines. Some characteristic chemical peaks on ^{1}H–NMR spectra were summarized in Table **1**. Elemental analysis of all compounds **1–2** was performed.

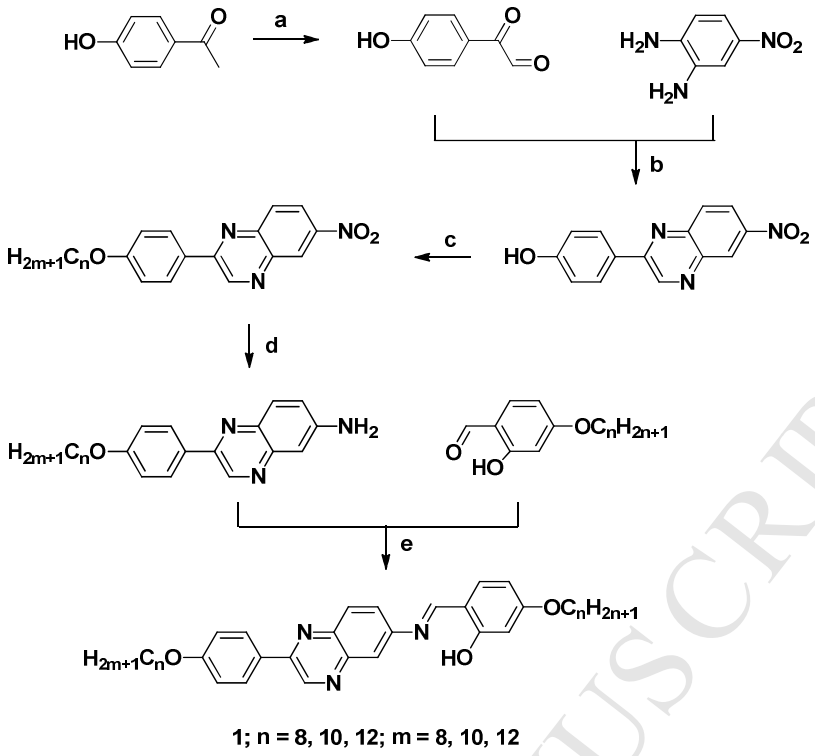

1; n = 8, 10, 12; m = 8, 10, 12

Scheme 1. Reagents and conditions. (a) SeO_2, refluxing in 1,4-dioxane/H_2O (20/1), 4 h (b) AcOH, refluxing in ethanol, 8 h (c) K_2CO_3, $C_nH_{2n+1}Br$, refluxing in DMSO, 24 h (d) Pd/C, hydrazine monohydrate, refluxing in EtOH, 6 h (e) AcOH, refluxing in THF, 24 h.

Table 1. The characteristic chemical peaks[a] on ^{1}H NMR spectra for compounds **1–2**

Compds	**1**	**2a**	**2b**
–O*H* (phenolic)	13.40–13.51	7.54	–
–N=C*H*– (imine)	8.67–8.68	–	–
–C*H*=N– (imine)	–	8.79–8.82	8.70

[a]: samples were all dissolved in $CDCl_3$ at rt. Unit: δ (ppm).

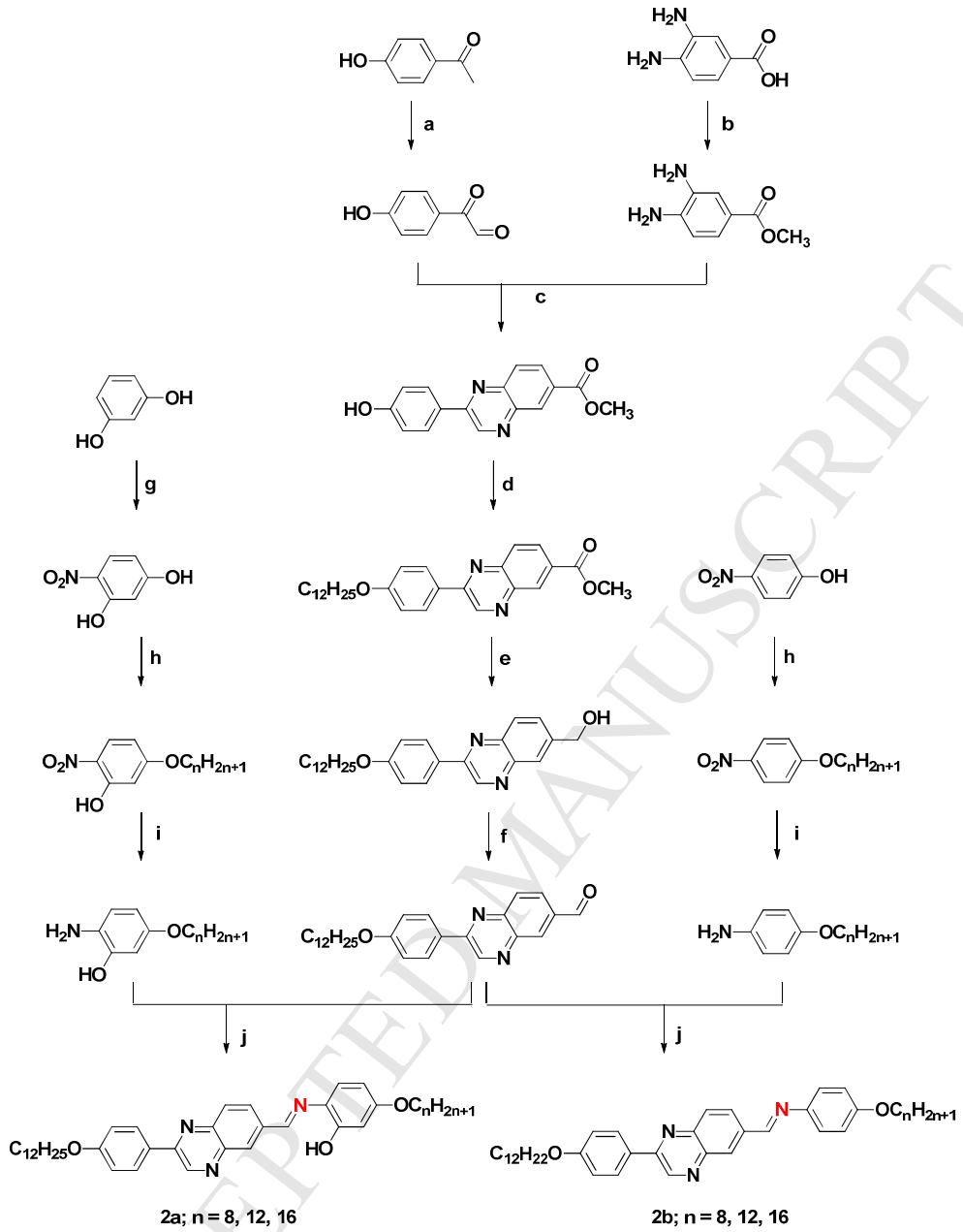

Scheme 2. Reagents and conditions. (a) SeO_2, refluxing in 1,4-dioxane/H_2O = 20/1, 4 h (b) 95% H_2SO_4 (drops), refluxing in MeOH, 4 h (c) refluxing in AcOH, 8 h (d) $C_{12}H_{25}Br$, K_2CO_3 and KI, refluxing in dry acetone, 24 h (e) LiAlH, stirred in dry THF, 6 h (f) Pyridinium chlorochromate, stirred in dry THF, 4 h (g) $C_nH_{2n+1}Br$, K_2CO_3 and KI, refluxing in dry acetone, 24 h (h) 65% HNO_3, refluxing in CH_2Cl_2, 1 h (i) Pd/C, hydrazine monohydrate, EtOH, reflux, 6 h (j) AcOH, refluxing in EtOH, 24 h.

In order to identify the formation of H–bonds possibly formed in crystal, liquid crystal or/and isotropic states, variable temperature FT–IR spectra of three compounds **1**–**2** (all m, n = 12) were performed (in Fig. 2). In this experiment, a thin disc grounded with KBr was prepared and studied at a temperature of 30 to 250 °C on the heating process. In general, the IR frequency

of intermolecular H–bonds formed by phenolic–OH group occurred at ca. 3,200–3,400 cm^{-1}, whereas, intramolecular H–bonds occurred at a lower region of ca. 2,800–3,100 cm^{-1}. As seen from Fig. 2, a characteristic broad and weak peak of H–bond occurred at ca. 3,435 cm^{-1}, assigned to the phenolic –OH group was observed for compound **2a** (m = n = 12) only at temperature of T = 30 °C. A very weak peak at T = 70 °C was barely observed. However, this weak peak was not seen at higher temperatures or isotropic state. This indicated that an intermolecular H–bond was only formed in crystal state for compounds **2a**. Other compounds **1** and **2b** have no intermolecular H–bonds formed in either crystal or mesogenic states. Obviously, the H–bonds were not the major force or interaction induing the mesophases in such system.

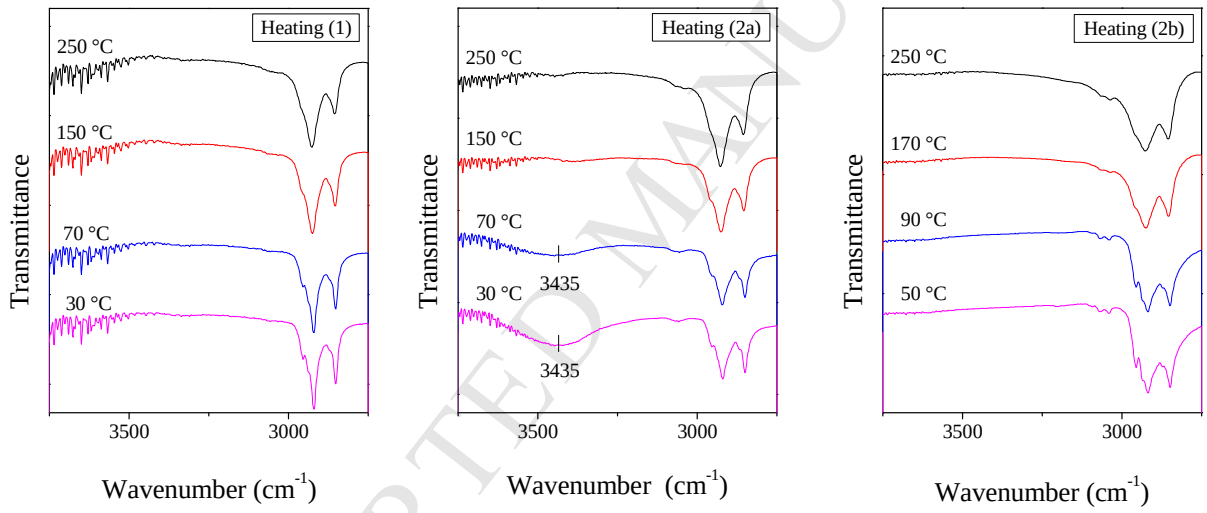

Fig. 2 Variable–temperature IR spectra for compound **1** (left), **2a** (middle) and **2b** (right, all m = n = 12) obtained in heating process using KBr pellets.

2.2 Single crystal structures of (E)-5-(octyloxy)-2-(((2-(4-(octyloxy)phenyl)quinoxalin-6-yl) imino)methyl)phenol and (E)-2-(((2-(4-(dodecyloxy)phenyl)quinoxalin-6-yl)methylene) amino)-5-(octyloxy)phenol

In order to understand the correlation between the molecular structures and the formation of mesophases, two single crystals of compounds **1** (m = n = 8) and **2a** (m = 12, n = 8) were obtained and their single crystallographic data were investigated. Two light yellow crystals

suitable for X–ray diffraction analysis were slowly grown from THF at room temperature. Fig. 3 shows the molecular structures with the atomic numberings, and Table 2 lists the crystallographic and structural refinement data for the two compounds. The crystal **1** crystallizes in the monoclinic space group P2(1)/c, with a = 27.627(2) Å, b = 10.3544(8) Å, c = 11.2292(9) Å, and Z = 4, in contrast, the crystal **2a** crystallizes in the triclinic space group P-1, with a = 5.7598(2)Å, b = 13.6324(4) Å, c = 24.1259(8) Å, and Z = 2. The overall structures of both crystals were quite planar, and the molecular lengths were *l* = 37.95 Å (atom C29–C37) and *l* = 42.76 Å (atom C29–C41), for crystal **1** and **2a**, respectively. On the other hand, the overall molecular planes in two crystals were quite planar, and the dihedral angles twisted from central plane 2 (see Fig. 4) to other phenyl or others were smaller than 8.839°. The relatively smaller dihedral angles favored the formation of mesophases induced in these two series of molecules. A summary of all dihedral angles in two crystals was listed in Table 3. The bond length of imine –CH=N was ranged in *d* = 1.2865 Å in crystal **1** and *d* = 1.2751 Å in crystal **2a**.

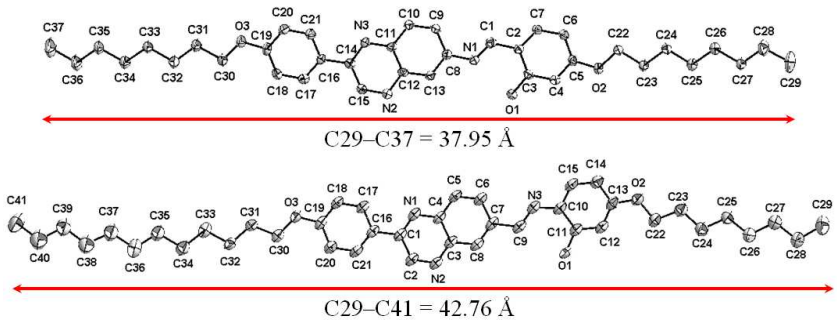

Fig. 3 Two ORTEP drawings for compound **1** (top) and **2a** (bottom) with the numbering scheme, and thermal ellipsoids of non–hydrogen atoms are drawn at the 50% probability level.

Table 2. Crystallographic data collected for single crystals **1** and **2a**.

Compd.	**1** (m = 8, n = 8)	**2a** (m = 12, n = 8)
Empirical formula	$C_{37}H_{47}N_3O_3$	$C_{41}H_{55}N_3O_3$
Formula weight	581.78	637.88
Temperature (K)	200(2)	200(2)
Crystal system	Monoclinic	Triclinic
Space group	P2(1)/c	P–1

a(Å)	27.627(2)	5.7598(2)
b(Å)	10.3544(8)	13.6324(4)
c(Å)	11.2292(9)	24.1259(8)
α(°)	90	102.2488(18)
β(°)	94.875(2)	93.2326(18)
γ(°)	90	99.4464(15)
Z	4	2
Density (calculated, Mg/m^3)	1.207	1.165
Crystal size (mm^3)	0.50x0.28x0.10	0.150x0.100x0.030
θ range for data collection(°)	0.74 to 27.50	3.373 to 67.500
Reflections collected	20512	12270
Independent reflections	7351 [R(int) = 0.0486]	6371 [R(int) = 0.0255]
Final R1, wR2	0.0660, 0.1456	0.0576, 0.1545

Table 3. Dihedral angles[a] twisted in **1** (m = 8, n = 8) and **2a** (m = 12, n = 8)

Ring plane	1	2	3	4
1	+8.839°	-	+0.410°	+6.517°
2a	+3.384°	-	+1.838°	+0.778°

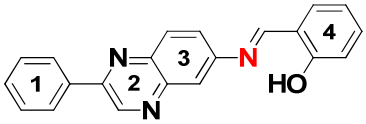

1

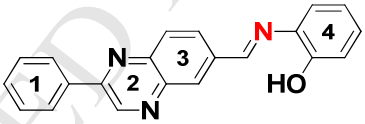

2a

[a]: angles are measured relative to central plane 2.

As expected, intramolecular H–bonds were observed in both crystal lattices. A distance of intramolecular H–bond, ca. *d* ~1.833, 2.131 and 2.574 Å was obtained for the two crystals, as shown Fig. 4. These intramolecular H–bonds kept the phenolic ring nearly coplanar to the quinoxaline ring, and the better planar structure was favorable for a better packing both in the solid or/and the liquid crystal state. In contrast, other intermolecular interactions, such as H–bonds, CH–π, and π–π were also observed in two crystals. In general, the CH–π[11], and π–π interactions were much weaker than H–bonds. However, these weak intermolecular forces were very crucial on the induction and/or formation of mesophases in such heterocyclic compounds. A

distance of *d* ~1.928–2.928 Å was observed for the intermolecular H–bonds in crystal **2a**. In contrast, other weaker intermolecular interactions of CH–π and π–π, at a distance of *d* ~ 2.812–3.403 Å were observed in both crystals. A dimeric structure was first formed by the intermolecular CH–π, and π–π interactions and the dimers were then packed into the lattice, shown in **Fig**. 6. A layer distance of ~30.33 Å was observed in lattice, which was smaller than those of *d* ~35–37 Å obtained by XRD diffraction at mesophases. In contrast, crystal **2a** has no strong H–bonds; a more coplanar core structure was instead facilitated by weaker intermolecular H–bonds; CH–O and CH–N. In crystal **2a**, the formation of a layered structure was formed or/and induced by strong H–bonds, OH–N (1.928 Å) and weaker H–bonds, CH–O (2.719 Å) and CH–N (2.928 Å), giving a head–to–tail arrangement in the lattice (Fig. 5). Neighboring layers were formed by weaker intermolecular CH–π (2.812 Å), shown in Fig 6. A summary of H–bonds and other interactions was listed in Table 4 and Table 5. All series of compounds **1** and **2** exhibited layered structure in mesophases. A layered structure correlated to the smectic phases in both unit cells was shown in **Fig**. 7.

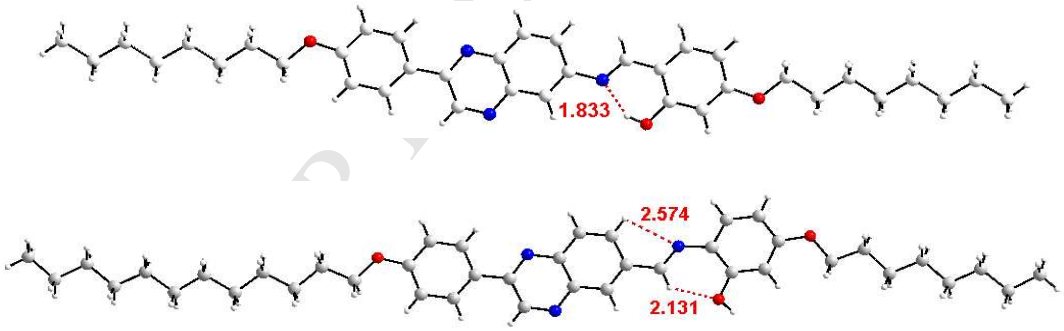

Fig. 4 Intramolecular H–bonds in crystals1 **1** (top) and **2a** (bottom).

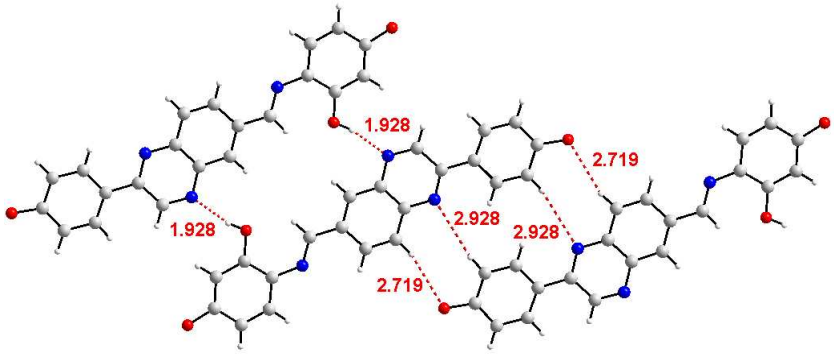

Fig. 5 Intermolecular H–bonds observed in crystal **2a** (m = 12, n = 8).

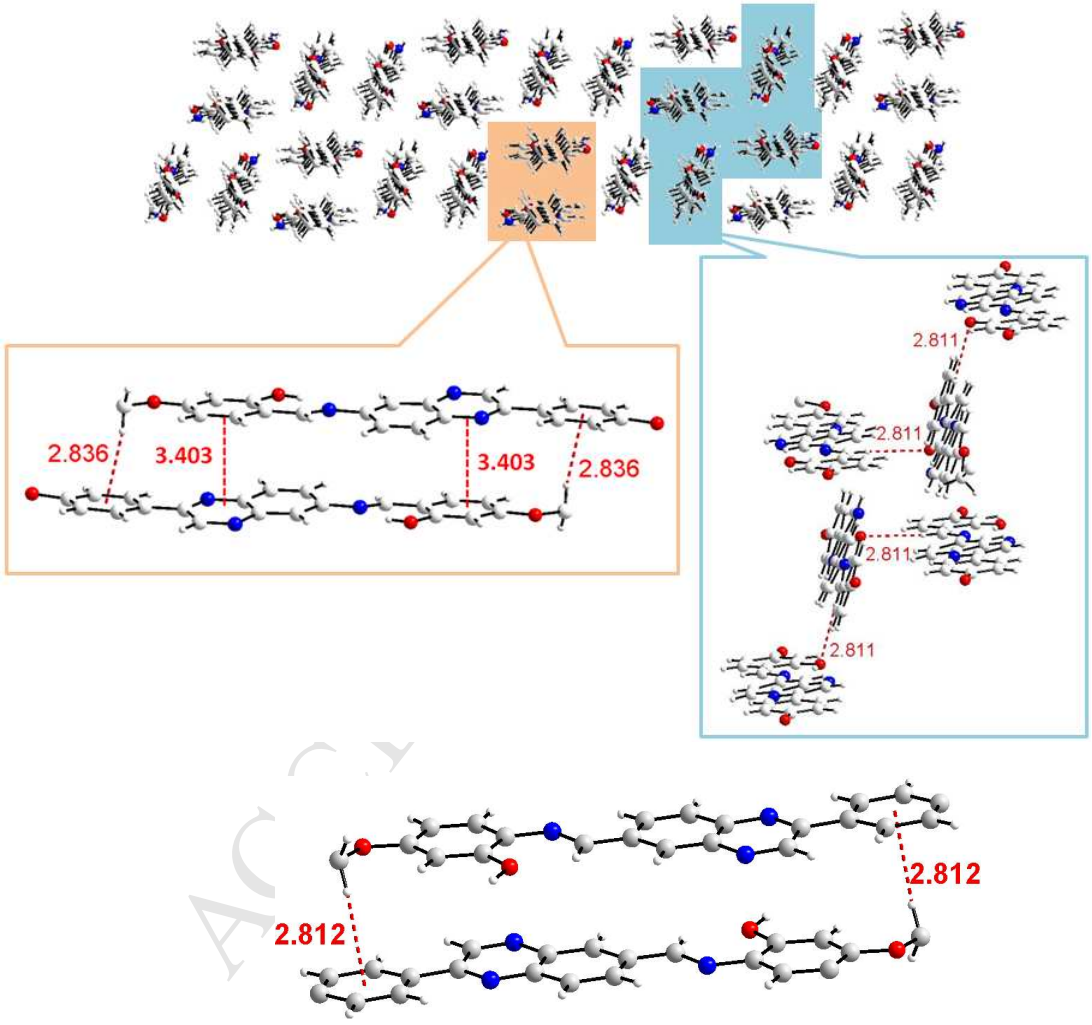

Fig. 6 Intermolecular CH–π, π–π interactions observed in crystal **1** (top) and **2a** (bottom).

Table 4. Intra and intermolecular H–bonds observed in both crystals.

Compd.	Type	no. H–bonds	bond distance/Å	angles/°
1	C–H…N	1	H1–N1 = 1.83	∠O1–H1–N1 = 147.00
2a	O–H…N	2	H1–N2 = 1.93	∠O1–H1–N2 = 166.90

Table 5. Weak interactions observed in **1** (m = 8, n = 8) and **2a** (m = 12, n = 8)

Compd.	Type	no. H–bonds	bond distance/Å	angles/°
1	C–H…O	2	2.81	∠C1–H1A–O1 = 158.51
	π…π	2	3.40	
	C–H…π	2	2.84	∠ring–H22B–C22 = 140.40
2a	C–H…O	1	H9–O1 = 2.13	∠C9–H9–O1 = 127.19
	C–H…O	2	H5–O3 = 2.72	∠C5–H5–O3 = 172.78
	C–H…N	1	H6–N3 = 2.57	∠C6–H6–N3 = 97.24
	C–H…N	2	H18–N1 = 2.93	∠C18–H18–N1 = 162.34
	C–H…π	2	ring–H22A = 2.81	∠ring–H22A–C22 = 154.23

* Interactions or distance measured from the center of ring to the atom.

** π–π interaction or distance measured from vertical distance from ring center of benzene to plane by quinoxaline.

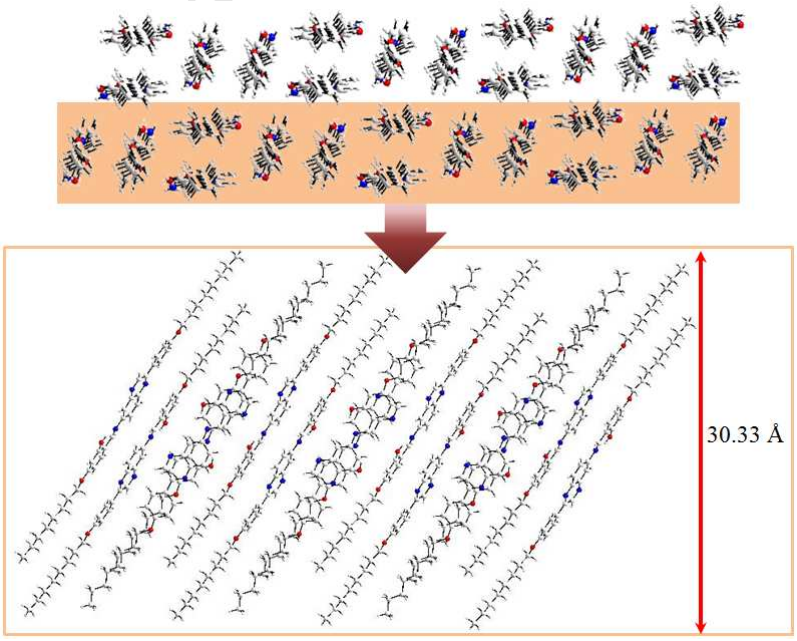

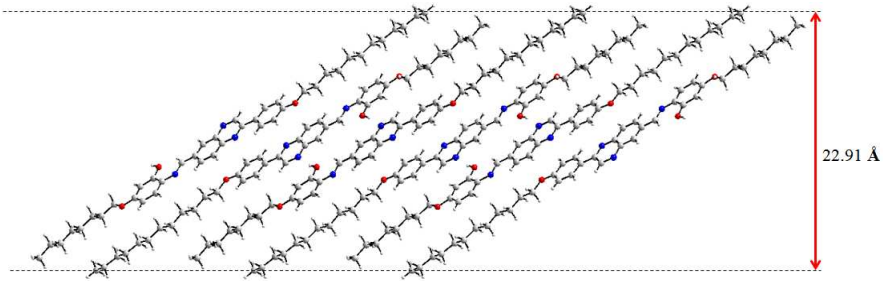

Fig. 7 A layer structure correlated to the smectic phases in **1** (top) and **2a** (bottom).

2.3. Thermal analysis and phase properties

The liquid crystalline behavior of Schiff–base derivatives **1–2** was characterized and studied by differential scanning calorimetry (DSC) and polarized optical microscope (POM). The phase transitions and thermodynamic data are summarized in Table 6. All three series of heterocyclic derivatives **1–2** exhibited an enanotropic mesomorphic behavior under POM observation, giving nematic/smectic C or smectic C phases. The sole shorter derivative **1** (m = n = 8) formed SmC phase at lower temperature and N phase at higher temperature. The clearing temperatures of compounds **1** decreased with carbon length of terminal alkoxy chains, i.e., T_{cl} = 274.8 (m = n = 8) > 261.9 (m = 12, n = 8) > 239.9 °C (m = 12, n = 16). The temperature range of mesophase was quite wide; ΔT_{meso} = 155.0 (m = 12, n = 16) < 189.4 (m = 12, n = 8) < 204.3 °C (m = n = 8) on cooling process. This wide range of mesophase temperature might be attributed to a better planar core, discussed in the crystallographic data. The transition enthalpies of SmC–to–I transitions were in the range of $\Delta H_{SmC \rightarrow I}$ = 10.6–17.8 kJ/mol. These compounds **1** have a higher clearing temperature than that of compounds **2a** and **2b**, for example, T_{cl} = 261.9 (**1**; m = 12, n = 8) > 256.7 (**2a**; m = 12, n = 8) > 245.7 °C (**2b**; m = 12, n = 8). The polar imine –C=N group is generally considered as an electron–donating group, however, the quinoxaline is an electron–withdrawing moiety. The direction of polar imine group affected the overall molecular dipole. Under optical microscope, they all exhibited typical Schlieren textures of four or/and two brushes or focal–conics textures. Furthermore, the nematic phase showed slightly homeotropic

domains, whereas, the smectic C phases showed no homeotropic textures.

In order to understand the effect of the polar groups, i.e. imine (–CH=N) and hydroxyl (–OH) incorporated on the formation of mesophases, the compound **2a** and **2b** were prepared and their mesomorphic behavior was investigated. Compounds **1** and **2a** are in fact geometric isomers. However, the imine moiety (–CHN) in both series of compounds was reversely incorporated, and the local dipoles might alter the overall molecular polarization. The DSC data showed that the clearing temperatures of compounds **2a** decreased with carbon length of alkoxy chains, and they were slightly lower than those of compounds **1** by ca. ΔT_{cl} = 5.2 (m = 12, n = 8) – 8.3 °C (m = 12, n = 12). All compounds **2a** formed smectic C phases, and the temperature range of the SmC phases was ΔT = 187.0–156.8 °C on cooling process. All compounds **2a** exhibited typical focal conics textures. Their transition enthalpies of SmC–to–I transitions were slightly smaller than those of compounds **1**, i.e. ΔH = 6.48–9.15 kJ/mol.

On the other hand, all compounds **2b** exhibited an enantiotropic behavior, giving N and SmC phases. Their clearing temperatures were slightly lower than those of compounds **1** and **2a**. Compounds **2a** and **2b** have the molecular structures in which the polar imine group is positioned opposite direction of the quinoxaline ring. This might reduce the overall molecular dipole to some extent, leading to a difference in polarization and/or anisotropics. Furthermore, a lack of polar hydroxyl group incorporated in compounds **2b** was apparently unable to induce the possible intra or intermolcular H–bonds. DSC data indicated that all clearing temperatures of compounds **2b** were lower than those of compounds **2a** by ΔT_{cl} = 11.0 (m = 12, n = 8) – 6.5 °C (m = 12, n = 12). Also the temperature of mesophase phases were slightly narrower than those of compounds **2a** by ca. ΔT_{SmC} = 13.5 (m = 12, n = 12) – 17.0 °C (m = 12, n = 16). The lower clearing or/and narrower temperature of SmC phases were possibly attributed to the absence of a polar hydroxyl group. A similar texture identified as focal–conic and Schlieren textures for smectic C and N phases was observed under optical microscope (**Fig**. 8). The bar graph in Fig. 9 showed the temperature of mesophases of all compounds **1**–**2**.

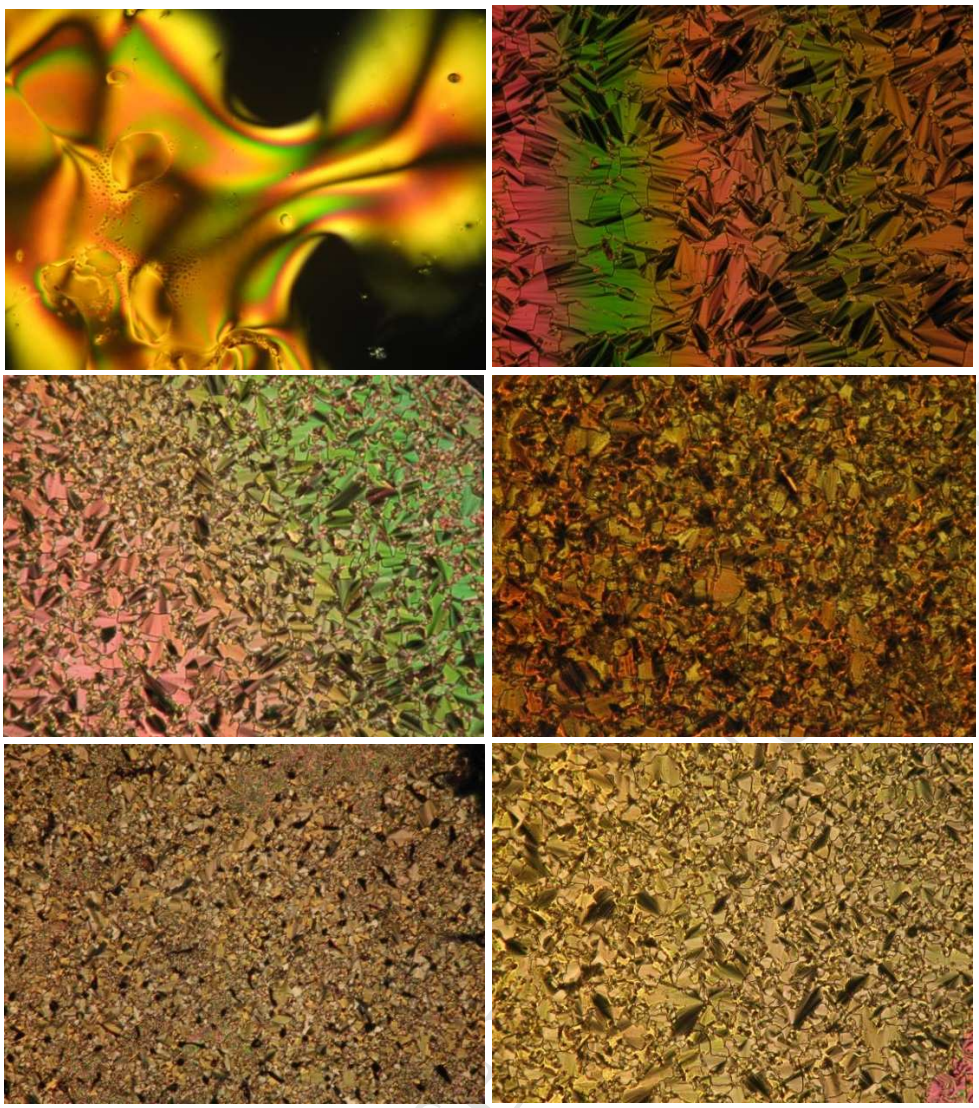

Fig. 8 Optical textures observed. N phase at 270 ^{o}C by **1** (m = 8, n = 8; top left), SmC phase at 240 ^{o}C by **1** (m = 8, n = 8; top right), SmC phase at 270 ^{o}C by **2a** (n = 8; middle left), SmC phase at 200 ^{o}C by **2a** (n = 12; middle right), SmC phase at 190 ^{o}C by **2a** (n = 16; bottom left), and SmC phase at 220 ^{o}C by **2b** (n = 16, bottom right).

Table 6. The phase temperatures and enthalpies[a] of the compounds 1-2.

1; m = 8, n = 8	Cr	105.9 (39.1) / 68.9 (32.1)	SmC	267.5 (5.41) / 265.3 (2.48)	N	274.8 (3.68) / 273.2 (2.59)	I			
10 10			Cr	93.2 (52.0) / 73.5 (53.9)	SmC	257.5 (17.8) / 254.8 (15.9)	I			
12 8			Cr	94.2 (31.4) / 71.1 (23.8)	SmC	261.9 (10.6) / 260.5 (9.42)	I			
12 12			Cr	102.5 (47.2) / 86.0 (46.0)	SmC	250.7 (12.9) / 249.0 (12.3)	I			
12 16			Cr	113.9 (66.6) / 83.1 (58.6)	SmC	239.9 (15.3) / 238.1 (14.0)	I			
2a; n = 8			Cr	104.0 (29.7) / 65.0 (37.0)	SmC	256.7 (6.48) / 252.0 (8.64)	I			
12			Cr	114.5 (40.2) / 61.6 (25.4)	SmC	242.4 (9.15) / 234.1 (4.87)	I			
16			Cr	117.7 (47.3) / 68.8 (31.2)	SmC	232.3 (7.40) / 225.6 (5.81)	I			
2b; n = 8	Cr	100.2 (39.6) / 74.2 (29.6)	SmC	239.2 (3.36) / 237.4 (3.01)	N	245.7 (1.71) / 244.4 (2.44)	I			
12	Cr	102.9 (41.0) / 76.2 (41.4)	SmC	235[a] / 234.4 (7.47)	N	235.9 (9.82) / 235.2 (2.03)	I			
16	Cr_1	87.3 (11.7) / 74.0 (78.2)	Cr_2	103.7 (89.1) / 82.4 (1.55)	SmC	223.6 (12.9) / 222.2 (11.9)	I			

[a]: m, n are the carbon numbers of the terminal chains, Cr = crystal, SmC = smectic C, N = nematic and I = Isotropic phases. The temperatures were determined by DSC on the cooling process with a scan rate is 10.0 °C/min.

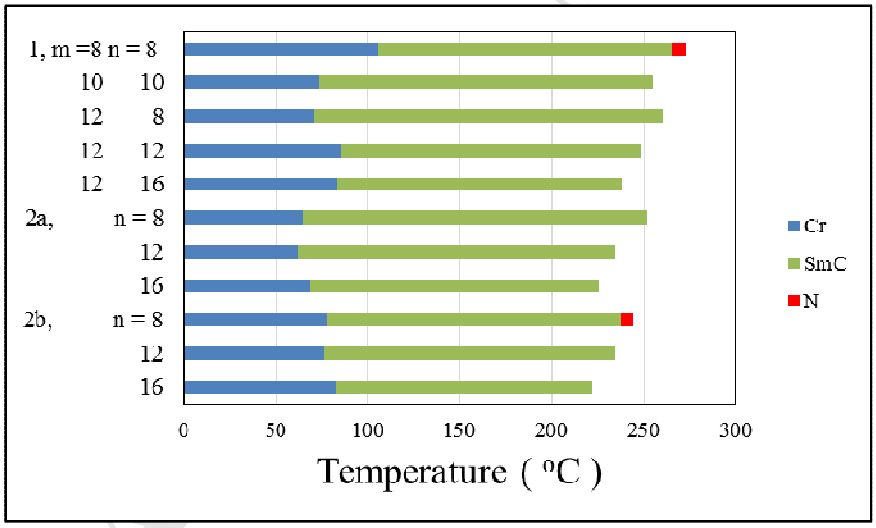

Fig. 9 Bar graphs showing the phase behavior of compounds **1–2**. All temperatures were taken from cooling process.

2.4 Variable powder diffraction

Variable–temperature powder XRD diffraction experiments were performed to confirm the

structures of the mesophases. Fig. 10 shows typical diffraction plots for three derivatives. A strong diffraction with a *d*–spacing of ca. ~35.6, Å, 37.1, Å and 36.4Å was obtained for compounds compound **1** (m = 12, n = 12), **2a** (m = 12, n = 12) and **2b** (m = 12, n = 12) at 180 ^{o}C, respectively. These three peaks corresponded to layer structures, assigned as Miller indices 001. These *d*–spacings were slightly larger than those of values measured from crystallographic data. In addition, a second diffraction peak at ~17.9 Å, 18.5 Å and 18.1 Å was also observed, assigned for indices 002. The diffraction patterns were typically characteristic of a layer structure observed for a SmC phase. The structure of SmC phase is similar to that of the unstructured SmA phase except that the long axes of the molecules are tilted with respect to the planes of the layers. The optical character is positive biaxial. The much smaller d–spacing indicated that the molecules were tilted or/and the terminal alkoxy chains were to some extent interdigitated in smectic C phase. Furthermore, a very broad and weak peak at ~ 4.70 Å was observed, and this peak was assigned to the molten alkoxy chains.

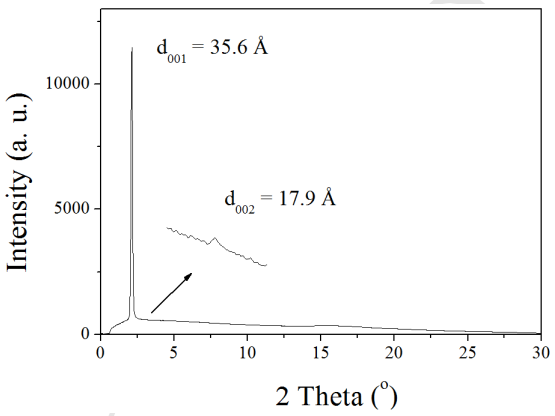

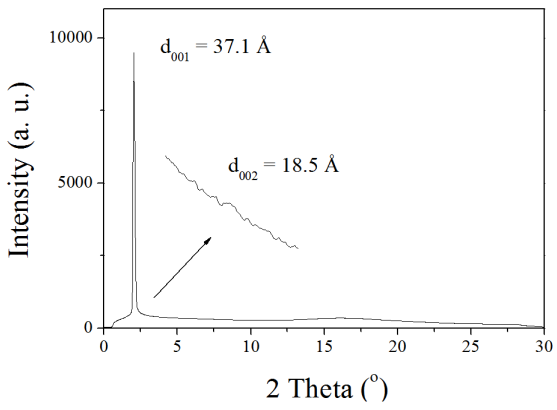

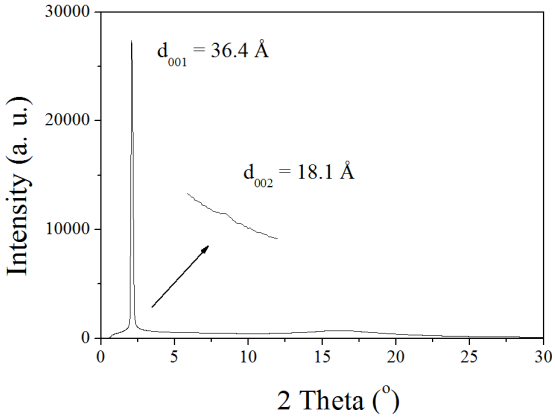

Fig. 10 The powder X–ray diffraction plots of compound **1** (m = n =12, top), **2a** (m = n = 12, middle) and **2b** (m = n = 12, bottom) at 180 °C

Table 7. Detailed indexation by powder XRD of smectic C phases[a] in compounds **1–2.**

Compds	Mesophases/temp	d–Spacing	Miller indices
1 (m =12, n = 12)	SmC at 180.0 °C	35.6	001
		17.9	002
		4.70	halo
2a (m =12, n = 12)	SmC at 180.0 °C	37.1	001
		18.5	002
		4.70	halo
2b (m =12, n = 12)	SmC at 180.0 °C	36.4	001
		18.1	002
		4.70	halo

[a]: temperature taken on the cooling process;

2.5 Optical properties

The UV–vis absorptions of three compounds in CH_2Cl_2 solution at room temperature are presented in Figure 11. The UV–vis absorption spectra of three compounds **1–2** (all m = 12, n = 16) were quite similar. A longer conjugated length was extended by imine moiety in all three compounds. The absorption λ_{max} peaks occurred at *ca*. 394 (for **1**), 407 (for **2a**) and 390 nm (for **2b**) were attributed to π–π* transitions[10] arising from quinoxaline moiety. Other peaks at 259–333 nm were originated from n–π transitions, as summarized in Table 8. The imine –C=N

group is polar and generally considered as an electron–donating group, however, the quinoxaline is an electron–withdrawing moiety. The push–pull effect by these two groups in compound **1** has caused absorption slightly red–shifted over other compounds **2**. In contrast, the presence of a hydroxyl group in compound **2a** caused an apparent shift (ca. 17 nm) on the λ_{max} absorption.

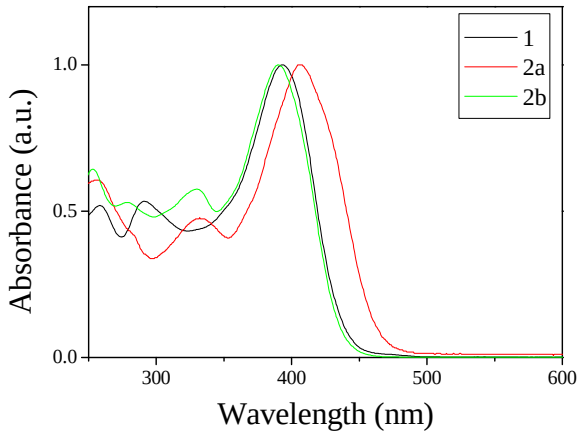

Fig. 11 Absorption spectra of the compounds **1** and **2a–b** (all m = 12, n = 16).

Table 8. Absorption data[a] of compounds **1** and **2a–b** (all m = 12, n = 16).

Compd	Absorption/nm
1	259, 291, 394
2a	258, 333, 407
2b	253, 279, 330, 390

[a]: Measured in CH_2Cl_2 solution (1.0×10^{-5} M) at room temperature.

3.0 Conclusions

Three series of heterocyclic quinoxaline Schiff bases were prepared and their mesomorphic properties studied. Inter or intramolecular H–bond, intermolecular CH–π and π–π played an important role in unit cells of crystals **1** and **2a**. They exhibited N/SmC or SmC phases over a wide range of mesophases. The compounds **1** and **2a** with a hydroxyl group incorporated have a slightly higher clearing temperature that the others, i.e. compounds **2b**. In addition, the polar

direction of the imine moiety also affected the mesophase temperatures.

4.0 Experimental Section

4.1 General materials and methods

All chemicals and solvents were reagent grades from Aldrich Chemical Co., and solvents were dried by standard techniques. ^{1}H and ^{13}C NMR spectra were measured on a Bruker DRS−300. DSC thermographs were carried out on a Mettler DSC−822 and calibrated with a pure indium sample. All phase transitions are determined by a scan rate of 10.0 °C/min. Optical polarized microscopy was carried out on Zeiss Axioplan 2 equipped with a hot stage system of Mettler FP90/FP82HT. The UV−vis absorption spectra were obtained using a Jasco V−530 spectrometer. Elemental analyses were performed on a Heraeus CHN−O−Rapid elemental analyzer. The powder diffraction data were collected from the Wiggler−A beam line of the National Synchrotron Radiation Research Center (NSRRC) with a wavelength of 1.3263 Å. The powder samples were charged in Lindemann capillary tubes (80 mm long and 0.01 mm thick) with an inner diameter of 1.0 mm from Charles Supper Co. The compounds of 4-alkoxynitro benzenes, 4-alkoxyanilines, 3-alkoxy-6-nitrophenols and 3-alkoxy-6-anilines were prepared by literatures' procedures.

4.2. 2-(4-Hydroxyphenyl)-2-oxoacetaldehyde

To a solution of SeO_2 (1.11 g, 0.01 mol), 1,4-dioxane/H_2O (20 : 1), 1-(4-hydroxyphenyl)ethanone (1.36 g, 0.01 mol) was added and the mixture was refluxed under nitrogen for 4 h. The solid residues were removed by filtration. The solvent of filtrate were removed under reduced pressure. The suspension was added 20 mL more water and heated to reflux for 3 h. Charcoal was added to the solution, and the solution was then refluxed for further 30 min. Upon cooling to room temperature, the solids were filtered. The filtrate was extracted by ethyl acetate/H_2O. The organic layer was collected and evaporated to dryness. The products isolated as pale yellow powder were obtained by recrystallization from CH_2Cl_2. Yield: 80% ^{1}H NMR (300 MHz, $CDCl_3$): δ 5.60−5.65

(m, 2H, CH–OH), 6.68 (s, 1H, –CH), 6.79–6.93 (m, 2H, Ar–H), 7.90–8.00 (m, 2H, Ar–H), 10.44 (s, 1H, –CH), 10.76 (s, 1H, Ar–OH). ^{13}C NMR (75 MHz, DMSO): δ 15.47, 18.72, 56.54, 62.64, 88.60, 94.73, 115.54, 115.58, 115.94, 116.03, 116.32, 125.35, 132.33, 162.67, 162.80, 193.01, 194.77.

4.3. Methyl 3,4-diaminobenzoate

To a solution of 3,4-diaminobenzoic acid (10.0 g, 0.07 mol) and 200 mL of MeOH, sulfuric acid (30 mL) was added dropwise. After refluxing for 24 h, the solution was cooled to room temperature. The organic solvent was removed with reduced pressure. The crude product was neutralized by aqueous K_2CO_3 then extracted by ethyl acetate/H_2O. The organic layers were collect and the solvent was evaporated to dryness. The products isolated as brown powder was obtained after recrystallization from MeOH. Yield: 78%. ^{1}H NMR (300 MHz, $CDCl_3$): δ 3.52 (s, 4H, NH_2), 3.82 (s, 3H, $–CH_3$), 6.64 (d, 1H, Ar–H, *J* = 8.1 Hz), 7.38 (d, 1H, Ar–H, *J* = 1.8 Hz), 7.44 (d, 1H, Ar–H, *J* = 9.9 Hz). ^{13}C NMR (75 MHz, DMSO): δ 51.62, 114.86, 118.31, 121.03, 123.22, 133.08, 140.39, 167.33.

4.4. Methyl 2-(4-hydroxyphenyl)quinoxaline-6-carboxylate

To a solution of methyl 3,4-diaminobenzoate (10.0 g, 0.07 mmol) and 200 mL of EtOH, 2-(4-hydroxyphenyl)-2-oxoacetaldehyde (9.0 g, 0.06 mmol) was added, the mixture was refluxed for 3 h. Upon cooling to room temperature, the crude product was collected by filtration. The products isolated as yellow powder were obtained after recrystallization from hexane/methanol. Yield: 90%. ^{1}H NMR (300 MHz, DMSO): δ 3.94 (s, 3H, $–OCH_3$), 6.97 (d, 2H, Ar–H, *J* = 8.7 Hz), 8.12 (d, 1H, Ar–H, *J* = 8.1 Hz), 8.23 (d, 2H, Ar–H, *J* = 12.3 Hz), 8.54 (d, 1H, Ar–H, *J* = 1.2 Hz), 9.56 (s, 1H, Ar–H), 10.18(s, 1H, Ar–H). ^{13}C NMR (75 MHz, DMSO): δ 53.07, 116.55, 126.78, 129.76, 129.95, 130.06, 131.15, 140.05, 144.17, 145.19, 153.03, 160.95, 166.03.

4.5. Methyl 2-(4-(dodecyloxy)phenyl)quinoxaline-6-carboxylate (m = 12)

Under nitrogen atmosphere, the mixture of methyl 2-(4-hydroxyphenyl)quinoxaline-6-carboxylate (0.5 g, 2 mmol), dry acetone (75 mL) , K_2CO_3 (0.37 g, 2 mmol) and KI (catalyst

amount) was refluxed for 24 h. The solids were filtered and the filtrate was concentrated by rotary evaporator. The crude product was extracted by ethyl acetate/H_2O. Organic layers were collected and dried over $MgSO_4$. The solvents were removed. The products isolated as white solids were obtained after recrystallization from hexane/MeOH. Yield 74 %. ^{1}H NMR (300 MHz, $CDCl_3$): δ 0.86 (t, 3H, –CH_3, *J* = 6.6 Hz), 1.25–1.49 (m, 18H, –CH_2), 1.77–1.84 (m, 2H, –CH_2), 4.00 (s, 3H, –OCH_3), 4.04 (t, 2H, –OCH_2, *J* = 6.45 Hz), 7.06 (d, 2H, Ar–H, *J* = 8.7 Hz), 8.13 (d, 1H, Ar–H, *J* = 8.4 Hz), 8.19 (d, 2H, Ar–H, *J* = 8.7 Hz), 8.33 (d, 1H, Ar–H, *J* = 8.7 Hz), 8.78 (s, 1H, Ar–H), 9.35 (s, 1H, Ar–H). ^{13}C NMR (75 MHz, $CDCl_3$): δ 14.07, 22.65, 25.99, 29.16, 29.31, 29.36, 29.56, 31.61, 31.88, 52.48, 68.25, 115.19, 128.31, 129.22, 129.46, 129.73, 130.19, 131.68, 140.28, 143.93, 144.38, 152.77, 161.61, 166.30. MS(FAB): calcd. For M+ $C_{28}H_{36}N_2O_3$: 448.27, found: 448.2718

4.6. (2-(4-(Dodecyloxy)phenyl)quinoxalin-6-yl)methanol (m = 12)

Under nitrogen atmosphere, to the mixture of methyl 2-(4-(dodecyloxy)phenyl)quinoxaline-6-carboxylate (0.5 g, 1 mmol) and 50 ml dry THF, lithium aluminium hydride (0.12 g, 3 mmol) was added. The mixture was stirred at room temperature for 4 h. Hydrochloric acid (2.0 N) was slowly added into the mixture for quenching the reaction. The mixture was concentrated by rotary evaporator and the residues were extracted with dichloromethane/H_2O. Organic layers were collected and dried over $MgSO_4$. The solvents were removed. The products isolated as white solids were purified by column chromatography eluting with ethyl acetate and hexane. Yield 60%. ^{1}H NMR (300 MHz, $CDCl_3$): δ 0.86 (t, 3H, –CH_3, *J* = 6.9 Hz) 1.24–1.62 (m, 18H, –CH_2), 1.81 (quint, 2H, –CH_2, *J* = 6.3 Hz), 4.02 (t, 2H, –CH_2, *J* = 6.3 Hz), 4.91 (s, 2H, –CH_2), 7.03 (d, 2H, Ar–H, *J* = 8.0 Hz), 7.74 (d, 1H, Ar–H, *J* = 7.7 Hz), 8.02 (s, 1H, Ar–H), 8.06 (d, 1H, Ar–H, *J* = 8.7 Hz), 8.12 (d, 2H, Ar–H, *J* = 7.7 Hz), 9.23 (s, 1H, Ar–H). ^{13}C NMR (125 MHz, $CDCl_3$): δ 14.11, 22.68, 26.02, 29.20, 29.34, 29.39, 29.59, 29.63, 31.91, 64.77, 68.22, 115.12, 126.08, 128.87, 129.27, 129.54, 141.01, 141.81, 142.15, 143.20, 151.43, 161.09.

2-(4-(Dodecyloxy)phenyl)quinoxaline-6-carbaldehyde (m = 12)

Under nitrogen atmosphere, to the mixture of (2-(4-(dodecyloxy)phenyl)quinoxalin-6-yl) methanol (0.5 g, 2 mmol) and 50 mL dry THF, pyridinium chlorochromate (0.75 g, 3.5 mmol) was added. The mixture was stirred under room temperature for 3 h. The mixture was then condensed by rotary evaporator, purified by column chromatography with ethyl acetate and hexane. White powder was obtained with 85% yield. ^{1}H NMR (300 MHz, $CDCl_3$): δ 0.86 (t, 3H, $-CH_3$, J = 6.9 Hz) 1.25–1.59 (m, 18H, $-CH_2$), 1.82 (quint, 2H, $-CH_2$, J = 6.6 Hz), 4.04 (t, 2H, $-CH_2$, J = 6.5 Hz), 7.06 (d, 2H, Ar–H, J = 8.7 Hz), 8.19 (d, 1H, Ar–H, J = 2.5 Hz), 8.22 (d, 2H, Ar–H, J = 1.7 Hz), 8.53 (s, 1H, Ar–H), 9.38 (s, 1H, Ar–H), 10.23 (s, 1H, CO–H). ^{13}C NMR (125 MHz, $CDCl_3$): δ 14.06, 22.63, 25.96, 29.11, 29.33, 29.53, 29.59, 31.86, 68.25, 115.23, 127.11, 128.14, 129.30, 130.52, 134.48, 136.06, 140.69, 144.20, 145.57, 153.30, 161.75, 191.25.

4.9. 4-(6-Nitroquinoxalin-2-yl)phenol

A solution of 2–(4–hydroxyphenyl)–2–oxoacetaldehyde (0.2 g, 4.19 mmol), 4-nitrobenzene-1,2-diamine (0.64 g，4.19 mmol) and 75 mL EtOH was refluxed for 30 min under nitrogen. The mixture was extracted by CH_2Cl_2 and water. The organic layers were collected, dried over $MgSO_4$ and then concentrated under reduced pressure. The products isolated as pale yellow powder were obtained after recrystallization from hexanes and MeOH. Yield: 76%. ^{1}H NMR (300 MHz, $CDCl_3$): δ 7.03 (d, 2H, Ar–H, J = 8.7 Hz), 8.14–8.22 (m, 3H, Ar–H), 8.52 (dd, 1H, Ar–H, ^{3}J = 9.3 Hz, ^{4}J = 2.4 Hz), 8.98 (d, 1H, Ar–H, J = 2.4 Hz), 9.24 (s, 1H, Ar–H). ^{13}C NMR (125 MHz, DMSO): δ 116.15, 116.22, 123.78, 124.69, 124.88, 125.91, 129.66, 129.97, 130.60, 130.73, 139.08, 144.47, 145.94, 146.49, 153.42, 161.00.

4.10. 2-(4-(Octyloxy)phenyl)-6-nitroquinoxaline (m = 8)

Under nitrogen atmosphere, a mixture of 4-(6-nitroquinoxalin-2-yl)phenol (0.5 g, 2 mmol) and K_2CO_3 (0.37 g, 2.0 mmol) was mixed in 75 mL dry acetone. The solution was then refluxed for 30 min. The mixture was then added 1–bromooctane (0.39 g, 2.0 mmol) and further refluxed for 24 h. The residual solids were filtered off. The filtrate was extract by ethyl acetate/water. The organic layers were then collected and concentrated and then concentrated by rotary evaporator. The

products were purified by column chromatography eluting with ethyl acetate and hexane. Yellow powder; yield 70%. ^{1}H NMR (300 MHz, $CDCl_3$): δ 0.88 (t, 3H, $-CH_3$, J = 6.6 Hz), 1.17–1.55 (m, 10H, $-CH_2$), 1.82 (quint, 2H, $-CH_2$, J = 7.8 Hz), 4.05 (t, 2H, $-OCH_2$, J = 6.5 Hz), 7.07 (d, 2H, Ar–H, J = 8.9 Hz), 8.12–8.30 (m, 3H, Ar–H), 8.50 (dd, 1H, Ar–H, ^{3}J = 9.15 Hz, ^{4}J = 2.5 Hz), 8.97 (d, 1H, Ar–H, 2.1 Hz), 9.42 (s, 1H, Ar–H). ^{13}C NMR (125 MHz, $CDCl_3$): δ 14.23, 22.78, 26.14, 29.28, 29.36, 29.47, 31.93, 68.48, 115.49, 123.81, 125.73, 127.88, 129.65, 130.91, 139.95, 145.31, 147.10, 153.97, 162.25.

4.11. 2-(4-(Decyloxy)phenyl)-6-nitroquinoxaline (m = 10)

Yellow solids; yield 72%. ^{1}H NMR (300 MHz, $CDCl_3$): δ 0.87 (t, 3H, $-CH_3$, J = 4.2 Hz), 1.18–1.52 (m, 14H, $-CH_2$), 1.73–1.86 (m, 2H, $-CH_2$), 4.05 (t, 2H, $-OCH_2$, J = 6.3 Hz), 7.07 (d, 2H, Ar–H, J = 4.5 Hz), 8.17–8.23 (m, 3H, Ar–H), 8.50 (dd, 1H, Ar–H, ^{3}J = 9 Hz, ^{4}J = 2.4 Hz), 8.96 (d, 1H, Ar–H, 2.1 Hz), 9.42 (s, 1H, Ar–H). ^{13}C NMR (125 MHz, $CDCl_3$): δ 14.10, 22.66, 25.99, 29.14, 29.30, 29.37, 29.55, 31.88, 68.33, 115.34, 123.67, 125.59, 127.73, 129.51, 130.76, 139.80, 145.17, 146.95, 153.82, 162.10.

4.12. 2-(4-(Dodecyloxy)phenyl)-6-nitroquinoxaline (m = 12)

Yellow solids; yield 73%. ^{1}H NMR (300 MHz, $CDCl_3$): δ 0.86 (t, 3H, $-CH_3$, J = 6.6 Hz) 1.19–1.68 (m, 18H, $-CH_2$), 1.82 (quint, 2H, $-CH_2$, J = 6.6 Hz), 4.05 (t, 2H, $-CH_2$, J = 6.6 Hz), 7.07 (d, 2H, Ar–H, J = 4.2 Hz), 8.16–8.23 (m, 3H, Ar–H), 8.50 (d, 1H, Ar–H, J = 9.3 Hz), 8.96 (s, 1H, Ar–H), 9.41 (s, 1H, Ar–H). ^{13}C NMR (125 MHz, $CDCl_3$): δ 14.10, 22.68, 26.00, 29.15, 29.37, 29.58, 29.64, 31.91, 68.35, 115.35, 123.67, 125.59, 129.51, 130.77, 139.81, 145.16, 146.97, 153.82, 162.13.

4.13. (E)-5-(octyloxy)-2-(((2-(4-(octyloxy)phenyl)quinoxalin-6-yl)imino)methyl)phenol 1 (m = 8, n = 8)

To a solution of 2-hydroxy-4-(octyloxy)benzaldehyde (1.5 g, 6.0 mmol) dissolved in 50 mL THF, 2-(4-(octyloxy)phenyl)quinoxalin-6-amine (2.0 g, 5.7 mmol) was added, and the mixture was refluxed overnight. Methanol was slowly added to give brown solids. The crude product was

collected and then purified by recrystallization from dichloromethane and methanol. Yellow crystal, yield: 90%. ^{1}H NMR (300 MHz, $CDCl_3$): δ 0.86 (t, 6H, $-CH_3$, J = 4.2 Hz) 1.23–1.65 (m, 20H, $-CH_2$), 1.73–1.89 (m, 4H, $-CH_2$), 3.94–4.10 (m, 4H, $-OCH_2$), 6.48–6.56 (m, 2H, Ar–H), 7.05 (d, 2H, Ar–H, J = 4.8 Hz), 7.29 (d, 1H, Ar–H, J = 4.8 Hz), 7.68 (d, 1H, Ar–H, J = 5.4 Hz), 7.83 (s, 1H, Ar–H), 8.09 (d, 1H, Ar–H, J = 5.1 Hz), 8.14 (d, 2H, Ar–H, J = 4.8 Hz), 8.67 (s, 1H, –CH=N), 9.25 (s, 1H, Ar–H), 13.40 (s, 1H, Ar–H). ^{13}C NMR (125 MHz, $CDCl_3$): δ 13.96, 22.58, 25.96, 26.02, 29.07, 29.16, 29.22, 29.27, 29.31, 31.77, 68.30, 68.39, 101.73, 107.98, 113.08, 115.22, 118.31, 125.78, 128.79, 129.09, 130.35, 133.90, 141.19, 141.93, 143.56, 149.16, 150.86, 161.16, 162.73, 164.06, 164.22, 176.61. Anal. Calcd for $C_{37}H_{47}N_3O_3$: C, 76.38; H, 8.14. Found C, 76.28; H, 8.11.

4.13.1 (E)-5-(decyloxy)-2-(((2-(4-(decyloxy)phenyl)quinoxalin-6-yl)imino)methyl)phenol 1 (m = 10, n = 10)

^{1}H NMR (300 MHz, $CDCl_3$): δ 0.87 (t, 6H, $-CH_3$, J = 6.6 Hz), 1.15–1.56 (m, 28H, $-CH_2$), 1.70–1.86 (m, 4H, $-CH_2$), 3.95–4.0 (m, 4H, $-OCH_2$), 6.43–6.58 (m, 2H, Ar–H), 7.05 (d, 2H, Ar–H, J = 8.7 Hz), 7.31 (d, 1H, Ar–H, J = 9.3 Hz), 7.70 (dd, 2H, Ar–H, ^{3}J = 8.7 Hz, ^{4}J = 2.1 Hz), 7.84 (d, 1H, Ar–H, J = 2.1 Hz), 8.07–8.19 (m, 3H, Ar–H), 8.68 (s, 1H, –CH=N), 9.27 (s, 1H, Ar–H), 13.51 (s, 1H, Ar–H). ^{13}C NMR (125 MHz, $CDCl_3$): δ 14.03, 22.67, 26.02, 26.08, 29.14, 29.31, 29.37, 29.41, 29.56, 31.31, 28.38, 68.46, 101.81, 108.07, 113.15, 115.30, 118.38, 125.87, 128.87, 129.18, 130.44, 133.97, 141.27, 142.02, 143.66, 149.28, 150.96, 161.24, 162.84, 164.13, 164.31. Anal. Calcd for $C_{41}H_{55}N_3O_3$: C, 77.20; H, 8.69. Found C, 77.12; H, 8.74.

4.13.2 (E)-2-(((2-(4-(dodecyloxy)phenyl)quinoxalin-6-yl)imino)methyl)-5-(octyloxy)phenol 1 (m = 12, n = 8)

^{1}H NMR (500 MHz, $CDCl_3$): δ 0.86 (t, 3H, $-CH_3$, J = 6.7 Hz), 1.25–1.44 (m, 28H, $-CH_2$), 1.75–1.83 (m, 4H, $-CH_2$), 3.98 (m, 4H, $-OCH_2$), 6.50 (m, 2H, Ar–H), 7.04 (d, 2H, Ar–H, J = 8.5 Hz), 7.31 (d, 1H, Ar–H, J = 8.7 Hz), 7.69 (d, 1H, Ar–H, J = 7.9 Hz), 7.83 (s, 1H, Ar–H), 8.09 (d, 1H, Ar–H, J = 8.8), 8.13 (d, 2H, Ar–H, J = 8.5 Hz), 8.67 (s, 1H, Ar–H), 9.26 (s, 1H, Ar–H),

13.52 (s, 1H, OH). ^{13}C NMR (75 MHz, $CDCl_3$): δ 14.08, 14.10, 22.63, 22.67, 25.96, 26.00, 29.02, 29.18, 29.19, 29.29, 29.33, 29.38, 29.55, 29.57, 29.61, 29.64, 31.78, 31.89, 68.19, 68.32, 101.51, 108.00, 112.92, 115.10, 118.23, 125.91, 128.78, 128.89, 130.30, 133.93, 141.11, 141.79, 143.60, 149.04, 161.04, 162.77, 163.96, 164.10. Anal. Calcd for $C_{41}H_{55}N_3O_3$: C, 77.20; H, 8.69. Found C, 76.50; H, 8.66.

4.13.3. (E)-5-(dodecyloxy)-2-(((2-(4-(dodecyloxy)phenyl)quinoxalin-6-yl)imino)methyl) phenol 1 (m = 12, n = 12)

^{1}H NMR (300 MHz, $CDCl_3$): δ 0.87(t, 6H, –CH_3, *J* = 4.2 Hz) 1.19–1.68 (m, 36H, –CH_2), 1.70–1.91 (m, 4H, –CH_2), 3.92–4.16 (m, 4H, –OCH_2), 6.48–6.52 (m, 2H, Ar–H), 7.05 (d, 2H, Ar–H, *J* = 8.1 Hz), 7.31 (d, 1H, Ar–H, *J* = 9.3 Hz), 7.70 (d, 2H, Ar–H, *J* = 6.9 Hz), 7.84 (s, 1H, Ar–H), 8.07–8.19 (m, 3H, Ar–H), 8.68 (s, 1H, –CH=N), 9.27(s, 1H, Ar–H), 13.50 (s, 1H, Ar–H). ^{13}C NMR (125 MHz, $CDCl_3$): δ 22.83, 26.18, 16.23, 29.29, 29.44, 29.49, 29.52, 29.57, 29.76, 29.79, 29.82, 32.09, 68.53, 68.61, 101.96, 108.21, 113.30, 115.45, 118.53, 126.00, 129.02, 129.32, 130.58, 134.12, 141.42, 142.15, 143.78, 149.39, 151.09, 161.39, 162.96, 164.28, 164.46. Anal. Calcd for $C_{45}H_{63}N_3O_3$: C, 77.88; H, 9.15. Found C, 77.82; H, 9.15.

4.13.4 (E)-2-(((2-(4-(dodecyloxy)phenyl)quinoxalin-6-yl)imino)methyl)-5-(hexadecyloxy) phenol 1 (m = 12, n = 16)

^{1}H NMR (300 MHz, $CDCl_3$): δ 0.83 (t, 3H, –CH_3, *J* = 6.6 Hz), 1.24–1.53 (m, 44H, –CH_2), 1.74–1.86 (m, 4H, –CH_2), 3.98–4.06 (m, 4H, –OCH_2), 6.49–6.52 (m, 2H, Ar–H), 7.05 (d, 2H, Ar–H, *J* = 8.8 Hz), 7.31 (d, 1H, Ar–H, *J* = 9.3 Hz), 7.70 (dd, 1H, Ar–H, ^3J = 8.9 Hz, ^4J = 2.3 Hz), 7.84 (d, 1H, Ar–H, *J* = 2.3), 8.1 (d, 1H, Ar–H, *J* = 9.0), 8.14 (d, 2H, Ar–H, *J* = 8.9 Hz), 8.68 (s, 1H, Ar–H), 9.27 (s, 1H, Ar–H), 13.50 (s, 1H, OH). ^{13}C NMR (75 MHz, $CDCl_3$): δ 14.18, 22.82, 26.18, 26.23, 29.29, 29.50, 29.51, 29.56, 29.75, 29.81, 29.85, 32.09, 68.54, 68.62, 101.96, 108.22, 113.30, 115.46, 118.52, 126.01, 129.02, 129.33, 130.58, 134.11, 141.42, 142.16, 143.08, 149.43, 151.11, 161.39, 162.98, 164.28, 164.46. Anal. Calcd for $C_{49}H_{71}N_3O_3$: C, 78.46; H, 9.54. Found C, 78.48; H, 9.54.

4.14 (E)-2-(((2-(4-(dodecyloxy)phenyl)quinoxalin-6-yl)methylene)amino)-5-(octyloxy) phenol 2a (m = 12, n = 8)

To a solution of 2-amino-5-(octyloxy)phenol (1.0 g, 4.5 mmol) dissolved in 50 mL of EtOH, 2-(4-(dodecyloxy)phenyl)quinoxaline-6-carbaldehyde (2.0 g, 4.5 mmol) was added and the mixture was refluxed overnight. Upon cooling to room temperature, the crude product was collected by filtration and then purified by recrystallization from CH_2Cl_2/CH_3OH. Yellow solids; yield 90%. ^{1}H NMR (300 MHz, $CDCl_3$): δ 0.88 (t, 3H, $-CH_3$, J = 6.9 Hz), 1.25–1.54 (m, 28H, $-CH_2$), 1.73–1.86 (m, 4H, $-CH_2$), 3.96 (t, 2H, $-OCH_2$, J = 6.6 Hz), 4.04 (t, 2H, $-OCH_2$, J = 6.6 Hz), 6.49 (dd, 1H, Ar–H, ^3J = 8.6 Hz, ^4J = 2.7 Hz), 6.58 (d, 1H, Ar–H, J = 2.7 Hz), 7.06 (d, 2H, Ar–H, J = 8.9 Hz), 7.37 (d, 1H, Ar–H, J = 9.0 Hz), 7.54 (s, 1H, –OH), 8.13 (d, 1H, Ar–H, J = 8.8), 8.17 (d, 2H, Ar–H, J = 9.0 Hz), 8.32 (s, 1H, Ar–H), 8.41 (d, 1H, Ar–H, J = 8.8 Hz), 8.82 (s, 1H, –CH=N), 9.31 (s, 1H, Ar–H). ^{13}C NMR (75 MHz, $CDCl_3$): δ 14.11, 22.68, 26.04, 29.21, 29.36, 29.41, 29.60, 31.82, 31.92, 68.28, 68.34, 100.54, 107.48, 116.36, 127.88, 128.01, 128.69, 129.09, 129.99, 130.76, 136.80, 141.23, 143.75, 144.04, 151.72, 152.05, 154.27, 160.89, 161.43. Anal. Calcd for $C_{41}H_{55}N_3O_3$: C, 77.20; H, 8.69. Found C, 77.28; H, 8.73.

4.14.1(E)-5-(dodecyloxy)-2-(((2-(4-(dodecyloxy)phenyl)quinoxalin-6-yl)methylene)amino) phenol 2a (m = 12, n = 12)

Yellow solids, 88%.^{1}H NMR (300 MHz, $CDCl_3$): δ 0.86 (t, 3H, $-CH_3$, J = 6.9 Hz), 1.25–1.46 (m, 36H, $-CH_2$), 1.73–1.86 (m, 4H, $-CH_2$), 3.95 (t, 2H, $-OCH_2$, J = 6.6 Hz), 4.01 (t, 2H, $-OCH_2$, J = 6.6 Hz), 6.48 (dd, 1H, Ar–H, ^3J = 8.7 Hz, ^4J = 2.4 Hz), 6.57 (d, 1H, Ar–H, J = 2.7 Hz), 7.05 (d, 2H, Ar–H, J = 8.7 Hz), 7.36 (d, 1H, Ar–H, J = 9.0 Hz), 7.54 (s, 1H, –OH), 8.10 (d, 1H, Ar–H, J = 8.7), 8.17 (d, 2H, Ar–H, J = 8.4 Hz), 8.32 (s, 1H, Ar–H), 8.39 (d, 1H, Ar–H, J = 9.0 Hz), 8.79 (s, 1H, –CH=N), 9.29 (s, 1H, Ar–H). ^{13}C NMR (75 MHz, $CDCl_3$): δ 14.12, 22.69, 26.03, 29.21, 29.36, 29.40, 29.60, 29.65, 31.93, 68.28, 68.34, 100.54, 107.47, 115.22, 127.87, 128.00, 128.67, 129.07, 129.98, 130.76, 136.78, 141.23, 143.74, 144.03, 151.70, 152.04, 154.27, 160.89, 161.42. Anal. Calcd for $C_{41}H_{55}N_3O_3$: C, 77.88; H,9.15. Found C, 77.66; H,9.12.

4.14.2(E)-2-(((2-(4-(dodecyloxy)phenyl)quinoxalin-6-yl)methylene)amino)-5-(hexadecyloxy) phenol 2a (m = 12, n = 16)

Yellow solids, yield 85%. ^{1}H NMR (300 MHz, $CDCl_3$): δ 0.86 (t, 3H, –CH_3, *J* = 6.9 Hz), 1.25–1.46 (m, 44H, –CH_2), 1.75–1.84 (m, 4H, –CH_2), 3.95 (t, 2H, –OCH_2, *J* = 6.3 Hz), 4.04 (t, 2H, –OCH_2, *J* = 6.6 Hz), 6.48 (dd, 1H, Ar–H, ^{3}J = 9.0 Hz, ^{4}J = 2.7 Hz), 6.58 (d, 1H, Ar–H, *J* = 2.4 Hz), 7.06 (d, 2H, Ar–H, *J* = 8.7 Hz), 7.37 (d, 1H, Ar–H, *J* = 8.7 Hz), 7.54 (s, 1H, –OH), 8.13 (d, 1H, Ar–H, *J* = 8.7), 8.18 (d, 2H, Ar–H, *J* = 8.7 Hz), 8.34 (s, 1H, Ar–H), 8.41 (d, 1H, Ar–H, *J* = 9.9 Hz), 8.81 (s, 1H, –CH=N), 9.31 (s, 1H, Ar–H). ^{13}C NMR (75 MHz, $CDCl_3$): δ 14.10, 22.68, 26.02, 29.19, 29.39, 29.59, 29.67, 31.91, 68.25, 68.31, 100.51, 107.45, 115.19, 116.33, 127.83, 127.97, 128.64, 129.05, 129.95, 130.73, 136.75, 141.19, 143.70, 144.00, 151.65, 152.00, 154.65, 160.86, 161.40. Anal. Calcd for $C_{49}H_{71}N_3O_3$: C, 78.46; H, 9.54. Found C, 78.48; H, 9.35.

4.15 (E)-N-((2-(4-(dodecyloxy)phenyl)quinoxalin-6-yl)methylene)-4-(octyloxy)aniline 2b (m = 12, n = 8)

To a solution of 4-(octyloxy)aniline (1.0 g, 4.7 mmol) dissolved in 50 mL of EtOH, 2-(4-(dodecyloxy)phenyl)quinoxaline-6-carbaldehyde (2.0 g, 4.5 mmol) was added and the mixture was refluxed overnight. The crude product was collected by filtration and then purified by recrystallization from CH_2Cl_2/CH_3OH. Yellow solids; yield 90%. ^{1}H NMR (300 MHz, $CDCl_3$): δ 0.86 (t, 3H, –CH_3, *J* = 6.9 Hz), 1.25–1.55 (m, 28H, –CH_2), 1.74–1.86 (m, 4H, –CH_2), 3.98 (t, 2H, –OCH_2, *J* = 6.6 Hz), 4.04 (t, 2H, –OCH_2, *J* = 6.6 Hz), 6.94 (d, 2H, Ar–H, *J* = 8.9 Hz), 7.06 (d, 2H, Ar–H, *J* = 8.9 Hz), 7.31 (d, 2H, Ar–H, *J* = 8.9 Hz), 8.13 (d, 1H, Ar–H, *J* = 8.8 Hz), 8.18 (d, 2H, Ar–H, *J* = 8.9), 8.32 (d, 1H, Ar–H, *J* = 1.7 Hz), 8.48 (dd, 1H, Ar–H, ^{3}J = 8.7 Hz, ^{4}J = 1.8 Hz), 8.70 (s, 1H, –CH=N), 9.31 (s, 1H, Ar–H). ^{13}C NMR (75 MHz, $CDCl_3$): δ 14.10, 22.67, 26.05, 29.24, 29.29, 29.38, 29.64, 31.81, 31.91, 68.25, 68.31, 115.05, 115.18, 122.45, 128.12, 128.72, 129.04, 129.88, 131.15, 137.16, 141.19, 143.58, 143.99, 151.99, 156.41, 158.36, 161.35. Anal. Calcd for $C_{41}H_{55}N_3O_3$: C, 79.18; H, 8.91. Found C, 79.19; H, 8.91.

4.15.1 (E)-4-(dodecyloxy)-N-((2-(4-(dodecyloxy)phenyl)quinoxalin-6-yl)methylene) 2b

(m = n = 12)

Yellow solids; yield 85%. ^{1}H NMR (300 MHz, $CDCl_3$): δ 0.86 (t, 3H, –CH_3, *J* = 6.9 Hz), 1.25–1.59 (m, 36H, –CH_2), 1.74–1.86 (m, 4H, –CH_2), 3.97 (t, 2H, –OCH_2, *J* = 6.6 Hz), 4.04 (t, 2H, –OCH_2, *J* = 6.6 Hz), 6.94 (d, 2H, Ar–H, *J* = 8.9 Hz), 7.05 (d, 2H, Ar–H, *J* = 8.9 Hz), 7.30 (d, 2H, Ar–H, *J* = 8.9 Hz), 8.13 (d, 1H, Ar–H, *J* = 8.8 Hz), 8.17 (d, 2H, Ar–H, *J* = 8.9), 8.32 (d, 1H, Ar–H, *J* = 1.7 Hz), 8.48 (dd, 1H, Ar–H, ^{3}J = 8.8 Hz, ^{4}J = 1.8 Hz), 8.70 (s, 1H, –CH=N), 9.30 (s, 1H, Ar–H). ^{13}C NMR (75 MHz, $CDCl_3$): δ 14.12, 22.70, 26.06, 29.22, 29.36, 29.42, 29.66, 31.93, 68.28, 68.35, 115.08, 115.21, 122.46, 128.15, 128.76, 129.06, 129.90, 131.16, 137.20, 141.22 143.59, 144.11, 152.00, 156.40, 158.40, 161.38. Anal. Calcd for $C_{45}H_{63}N_3O_2$: C, 79.72; H, 9.37. Found C, 79.47; H, 9.30.

4.15.2 (E)-N-((2-(4-(dodecyloxy)phenyl)quinoxalin-6-yl)methylene)-4-(hexadecyloxy)aniline 2b (m = 12, n = 16)

^{1}H NMR (300 MHz, $CDCl_3$): δ 0.86 (t, 3H, –CH_3, *J* = 6.9 Hz), 1.25–1.55 (m, 44H, –CH_2), 1.74–1.86 (m, 4H, –CH_2), 3.97 (t, 2H, –OCH_2, *J* = 6.6 Hz), 4.04 (t, 2H, –OCH_2, *J* = 6.6 Hz), 6.94 (d, 2H, Ar–H, *J* = 8.7 Hz), 7.06 (d, 2H, Ar–H, *J* = 9.0 Hz), 7.31 (d, 2H, Ar–H, *J* = 8.7 Hz), 8.13 (d, 1H, Ar–H, *J* = 9.0 Hz), 8.18 (d, 2H, Ar–H, *J* = 9.0), 8.32 (d, 1H, Ar–H, *J* = 1.8 Hz), 8.34 (s, 1H, Ar–H), 8.49 (dd, 1H, Ar–H, ^{3}J = 8.7 Hz , ^{4}J = 1.8 Hz), 8.70 (s, 1H, –CH=N), 9.31 (s, 1H, Ar–H). ^{13}C NMR (75 MHz, $CDCl_3$): δ 14.10, 22.68, 26.03, 29.20, 29.35, 29.59, 29.66, 31.92, 68.27, 115.07, 115.20, 122.45, 128.14, 128.74, 129.06, 129.89, 131.51, 137.19, 141.20, 143.59, 144.09, 152.01, 156.42, 158.39, 161.37. Anal. Calcd for $C_{49}H_{71}N_3O_2$: C 80.47 ; H,9.75. Found C, 80.21; H,9.78.

Acknowledgements

We thank the Ministry of Science and Technology, Taiwan (MOST 104–2119–M–008–011) for generous support of this work. Also we deeply appreciated Prof. Hwo–Shuenn Sheu for performing powder XRD experiments at the National Synchrotron Radiation Research Center.

References:

1. (a) Kuo, H. M. ; Hsu, Y. T.; Wang, Y. W.; Lee, G. H.; Lai, C. K. *Tetrahedron* **2015**, *71*, 7729–7738; (b) Liu, T. M.; Lin, K. T.; Li, F. J.; Lee, G. H.; Chen, M. C.; Lai, C. K. *Tetrahedron* **2015**, *71*, 8649–8660; (c) Jacquemin, P. L.; Robeyns, K.; Devillers, M.; Garcia, Y. *Chem. Commun.* **2014**, *40*, 649–651; (d) Robert, F.; Jacquemin, P. L.; Tinant, B.; Garcia, Y. *RSC Adv*. **2013**, *3*, 6466–6471; (e) Francois, F.; Jacquemim, P. L.; Bernard, B.; Yann, G. *CrystEngComm* **2012**, *14*, 4396–4406; (f) Whiteoak, C. J.; Salassa, G.; Kleij, S. A. W. *Chem. Soc. Rev*. **2012**, *41*, 622–631; (g) Inokuma, Y.; Kawano, M.; Fujita, M. *Nat. Chem*. **2011**, *3*, 349–358; (h) Hadjoudis, E.; Chatziefthimiou, S. D.; Mavridis, I. M. *Curr. Org. Chem*. **2009**, *13*, 269–286; (i) Wezenberg, S. T.; Kleij, A. W. *Angew. Chem., Int. Ed*. **2008**, *47*, 2354–2364.

2. (a) Cao, X.; Jin, F.; Li, Y. F.; Chen, W. Q.; Duan, X. M.; Yang, L. M. *New J. Chem*. **2009**, *33*, 1578–1582; (b) Son, H. J.; Han, W. S.; Wee, K. R.; Yoo, D. H.; Lee, J. H.; Kwon, S. N.; Ko, J.; Kang, S. O. *Org. Lett*. **2008**, *10*, 5401–5404; (c) Xu, X.; Yu, G.; Chen, S.; Di, C.; Liu, Y. *J. Mater. Chem*. **2008**, *18*, 299–305; (e) Kulkarni, A. P.; Zhu, Y.; Babel, A.; Wu, P. T.; Jenekhe, S. *A. Chem. Mater*. **2008**, *20*, 4212–4223; (d) Chen, S.; Xu, X.; Liu, Y.; Qiu, W.; Yu, G.; Wang, H.; Zhu, D. *J. Phys. Chem. C* **2007**, *111*, 1029–1034; (e) Thomas, K. R. J.; Velusamy, M.; Lin, J. T.; Chuen, C. H.; Tao, Y. T. *Chem. Mater*. **2005**, *17*, 1860–1866.

3. (a) Qian, G.; Zhong, Z.; Luo, M.; Yu, D.; Zhang, Z.; Ma, D.; Wang, Z. Y. *J. Phys. Chem. C* **2009**, *113*, 1589–1595; (b) Wang, P.; Xie, Z.; Wong, O.; Lee, C. S.; Wong, N.; Hung, L.; Lee, S. *Chem. Commun*. **2002**, 1404–1405.

4. (a) Hu, T. S.; Lin, K. T. ; Mu, C. C.; Kuo, H. M.; Chen, M. C.; Lai, C. K. *Tetrahedron* **2014**, *70*, 9204–9213; (b) Lin, K. T. ; Kuo, H. M. ; Sheu, H. S.; Lai, C. K. *Tetrahedron* **2013**, *69*, 9045–9055; (c) Chen, C. J.; Wu, Y. C.; Sheu, H. S.; Lee, G. H.; Lai, C. K. *Tetrahedron* **2011**, *67*, 114–124; (d) Voisin, E.; Foster, E. J.; Rakotomalala, M.; Williams, V. E. *Chem. Mater*. **2009**, *21*, 3251–3261; (e) Koysal, O.; Okutan, M.; San, S. E.; Dincer, F.; Ahsen, V.; Durmus, D. *J. Phys. Chem. Solids*. **2009**, *70*, 266–271; (f) Foster, E. J.; Jones, R. B.; Lavigueur, C.; Williams, V. E. *J.*

Am. Chem. Soc. **2006**, 126, 8569−8574; (g) Foster, E. J.; Lavigueur, C.; Ke, Y. C.; Williams, V. E. *J. Mater. Chem*. **2005**, *15*, 4062−4068; (h) Bojinov, V. B.; Grabchev, I. K. *Org. Lett.* **2003**, *5*, 2185−2187.

5. Szydlowska, J.; Krzyczkowska, P.; Salamonczyk, M.; Gorecka, E.; Pociecha, D.; Maranowski, B.; Krowczynski, A. *J. Mater. Chem. C*, **2013**, *1*, 6883−6889.

6. Howard, M. J.; Heirtzler, F. R.; Dias, S. I. G. *J. Org. Chem. 2008, 73*, 2548−2533.

7. Chu, Y. Y.; Kuo, H. M. ; Wu, Y. C.; Wu, C. Y.; Sheu, H. S. ; Lee, G. H.; Chen, M. C.; Lai, C. K. *Tetrahedron* **2014**, *70*, 2389−2399.

8. Takeda, T.; Tsutsumi, J.; Hasegawa, T.; Noro, S. I.; Nakamura, T.; Akutagawa, T. *J. Mater. Chem. C*, **2015**, *3*, 3016−3022.

9. (a) Segura, J. L.; Juarez, R.; Ramos, M.; Seoane, C. *Chem. Soc. Rev*., **2015**, *44*, 6850−6885; (b) Sivadas, A. P.; Kumar, N. S. S.; Prabhu, D. D.; Varghese, S.; Prasad, S. K.; Rao, D. S. S.; Das, S. *J. Am. Chem. Soc*., **2014**, *136*, 5416−5423.

10. Wang, X.; Zhou, Y.; Lei, T.; Hu, N.; Chen, E. Q.; Pei, J. *Chem. Mater*., **2010**, *22*, 3735−3745.

11. (a) Ye, Q.; Chang, J.; Shao, J.; Chi, C. *J. Mater. Chem. C* **2012**, *22*, 13180−13186; (b) Goel, M.; Jayakannan, M. *Chem. Eur. J*. **2012**, *18*, 11987−11993; (c) Goel, M.; Jayakannan, M. *Chem. Eur. J*. **2012**, *18*, 2867−2874;